Muon-induced fission: A probe for nuclear dissipation and fission dynamics

V. E. Oberacker,[1,2] A. S. Umar,[1,2] J. C. Wells,[1,2,3]
C. Bottcher,[1,3] M. R. Strayer,[1,3] and J. A. Maruhn[1,4]
[1] *Center for Computationally Intensive Physics, Oak Ridge National Laboratory, Oak Ridge, Tennessee 37831*
[2] *Department of Physics and Astronomy, Vanderbilt University, Nashville, Tennessee 37235*
[3] *Physics Division, Oak Ridge National Laboratory, Oak Ridge, Tennessee 37831*
[4] *Institut für Theoretische Physik, Universität Frankfurt, D-6000 Frankfurt am Main, Germany*
(Received 17 March 1993)

Excited muonic atoms in the actinide region may induce prompt fission. Following atomic muon capture, some of the inner-shell transitions proceed by inverse internal conversion, i.e., the excitation energy of the muonic atom is transferred to the nucleus. In particular, the $(E2 : 3d \rightarrow 1s)$ muonic transition energy is close to the peak of the isoscalar giant quadrupole resonance in actinide nuclei which exhibits a large fission width. Prompt fission in the presence of a bound muon allows us to study the dynamics of large-amplitude collective motion. We solve the time-dependent Dirac equation for the muonic spinor wave function in the Coulomb field of the fissioning nucleus on a three-dimensional lattice and demonstrate that the muon attachment probability to the light fission fragment is a measure of the nuclear energy dissipation between the outer fission barrier and the scission point.

PACS number(s): 25.85.Ge, 36.10.Gv, 02.70.−c

I. INTRODUCTION

Nuclear physics experiments with μ^- beams provide information on fundamental symmetries and interactions. Moreover, muonic atoms have proven extremely useful in examining the electromagnetic properties of nuclei, e.g., electric charge distributions and multipole moments, because the muon has a high position probability density inside the nucleus owing to its small Compton wavelength $\lambda_C = \hbar/(m_\mu c) = 1.87$ fm [1,2]. In this paper we shall discuss how bound muons in muonic atoms may induce fission in actinide nuclei by inverse internal conversion and how muons may probe the dynamics of prompt fission because their mean lifetime exceeds the fission time scale by many orders of magnitude.

From a theoretical point of view, muon-induced fission has several attractive features. Because the nuclear excitation energy exceeds the fission barrier by several MeV, it is permissible to treat the fission dynamics classically (no barrier tunneling). The muon dynamics is determined by the electromagnetic interaction which is precisely known; hence, the process can be calculated, at least in principle, with any desired precision. Our main task is the solution of the Dirac equation for the muon in the presence of a time-dependent external Coulomb field which is generated by the fission fragments in motion. We will demonstrate that the muon attachment to the light fission fragment depends on the nuclear friction between the outer fission barrier and the scission point. In this context, nuclear friction is defined as the irreversible flow of energy (and linear or angular momentum) from collective to intrinsic single-particle motion [3]. We include in our classical dynamical calculations for the fission mode a linear friction force to account for energy dissipation via neutron and photon emission. Through muon-induced fission one expects to gain a deeper understanding of the energy dissipation mechanism in large-amplitude nuclear collective motion. A very important and still unresolved question in nuclear many-body theory is to what extent the dissipation mechanism can be understood in terms of "one-body friction" (collisions of the nucleons with the moving walls of the self-consistent mean field [4]) and the role played by "two-body friction" (two-body collisions between the nucleons).

Nonrelativistic calculations for muon-induced fission have been carried out by several theory groups [5–11], but only very recently have relativistic calculations become feasible [12,13]. We discuss here in detail our theoretical approach and the numerical implementation, and we wish to ultimately compare our results in detail with experimental data obtained at the Los Alamos Meson Physics Facility (LAMPF) [14–16], at CERN and the Paul Scherrer Institute (PSI) [17–20], and at the Tri-University Meson Facility (TRIUMF) [21,22].

II. PROMPT AND DELAYED FISSION INDUCED BY MUONS

Following the irradiation of a target with a μ^- beam the muons lose most of their kinetic energy by ionization in the target material within 10^{-9} to 10^{-10} s. Once their velocity has become comparable to the orbital electron velocities characteristic of these atoms, they are slowed down further by inelastic collisions with valence electrons and are finally captured into high-lying states ($n_\mu \approx 14$) forming a muonic atom. The theoretical aspects of the interaction of muons with condensed matter were first

studied by Fermi and Teller [23] and were later explored in more detail by Wu and Wilets [24] and by Kim [1]. Because all muonic bound states are unoccupied the muon will cascade down to the ground state within 10^{-13} s. From the outer shells the excited muonic atom decays preferentially by emission of Auger electrons. Since ΔE increases rapidly for the inner shells, the transitions between levels with $n \leq 5$ are dominated by mesic x rays. Alternatively, the transitions may proceed without emission of radiation via inverse internal conversion. From the K shell, the muon disappears at a characteristic rate $\lambda = \lambda_0 + \lambda_c$, where $\lambda_0 = (2.2 \times 10^{-6}\ \mathrm{s})^{-1}$ denotes the free leptonic decay rate and λ_c the nuclear capture rate; λ_c depends upon the charge and mass of the nucleus (Goulard-Primakoff formula [25]) and is of order $(7.5 \times 10^{-8}\ \mathrm{s})^{-1}$ for actinides [15]. Muons stopped in an actinide target may induce nuclear fission in two different ways.

(i) Delayed fission following nuclear muon capture. The muon is captured by a proton inside the nucleus and forms a neutron and a muon neutrino

$$\mu^- + (Z, A) \rightarrow (Z - 1, A)^* + \nu_\mu. \quad (1)$$

Even though most of the energy is taken away by the neutrino, the average nuclear excitation energy is $15 - 20$ MeV, which is well above the fission barrier for actinides $E_f = 5 - 6$ MeV. Fission via nuclear muon capture is *delayed*, i.e., it occurs with the characteristic mean lifetime of the weak decay process, $\tau_{\mathrm{capt}} = (7 - 8) \times 10^{-8}$ s.

(ii) Prompt fission resulting from inverse internal conversion in muonic atoms. In this case, the excitation energy of the muonic atom is transferred to the nucleus by an internal conversion process (nonradiative transition) and the muon ends up in the K shell of the muonic atom

$$(Z, A)(\mu^-)^* \rightarrow (Z, A)^* \mu^-. \quad (2)$$

For the innermost atomic transitions in an actinide muonic atom, the transition energy generally exceeds the fission barrier height. The result is *prompt fission in the presence of the muon*, since the muon is not annihilated by this process, in contrast to fission resulting from nuclear muon capture. The nucleus will be surrounded by the muon during the entire fission process, unless the muon is ionized. Eventually, the muon will decay by nuclear muon capture from the fission fragments. Experimentally, both fission modes can be distinguished because of their different time scale. In this paper, we focus on prompt muon-induced fission. This process was first discussed by Wheeler [26] and considered in more detail by Zaretski and Novikov [27]. It is important to know the specific atomic transitions that are responsible for prompt fission. Figure 1 shows the Coulomb interaction energy between the muon and a ^{238}U nucleus as well as the binding energies of the lowest bound states. Even though $E0$ transitions such as $2s \rightarrow 1s$ and $3s \rightarrow 1s$ exhibit the largest internal conversion rates they do not contribute to fission because they lead to excitation of the giant monopole resonance which is spherically symmetric and much too high in energy. On the other hand,

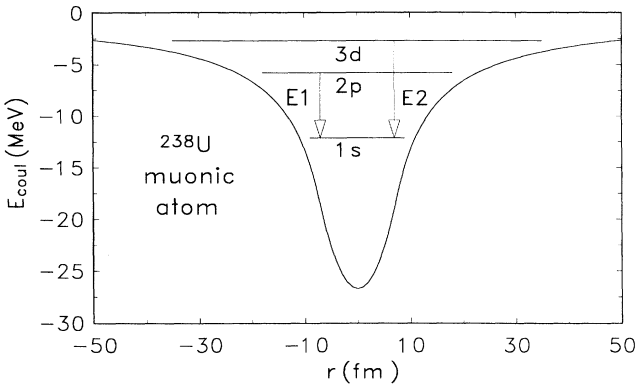

FIG. 1. Coulomb interaction potential and energy levels of the muonic atom $^{238}_{92}$U. Indicated are the two nonradiative muonic transitions leading to prompt muon-induced fission by inverse internal conversion ($E1 : 2p \rightarrow 1s, \Delta E = 6.6$ MeV) and ($E2 : 3d \rightarrow 1s, \Delta E = 9.6$ MeV).

the ($E1 : 2p \rightarrow 1s$) and the ($E2 : 3d \rightarrow 1s$) transitions result in excitation of the electric giant dipole and quadrupole resonances, respectively, both of which act as doorway states for fission; this is indicated schematically in Fig. 2. Let us consider the specific case of ^{238}U: The giant dipole resonance is located at $E_{\mathrm{GDR}} = 12.8$ MeV and has a width $\Gamma = 6$ MeV [28]; for the $T = 0$ giant quadrupole resonance the corresponding numbers are $E_{\mathrm{GQR}} = 9.9$ MeV and $\Gamma = 6.8$ MeV [29]. According to Teller and Weiss [30] it is very probable that the $3d \rightarrow 1s$ radiationless transition will be dominant for muon-induced fission, because its transition energy of 9.6 MeV is very close to the peak of the giant quadrupole resonance whereas the $2p \rightarrow 1s$ transition energy of 6.6 MeV is far off the center of the giant dipole resonance. Experimentally, the situation is controversial: Johansson *et al.* [18] measured muonic x rays in coincidence with prompt fission in ^{238}U. From the muonic x-ray intensity ratios for prompt and delayed fission they conclude that $(74 \pm 15)\%$ of all prompt events can be attributed to the $3d \rightarrow 1s$ radiationless transition and only $(26 \pm 15)\%$ to the $2p \rightarrow 1s$ transition. On the other hand, Kaplan *et al.* [22] find in similar studies a predominance of the $E1$ transitions in their prompt fission data.

The prompt muon-induced fission process is most eas-

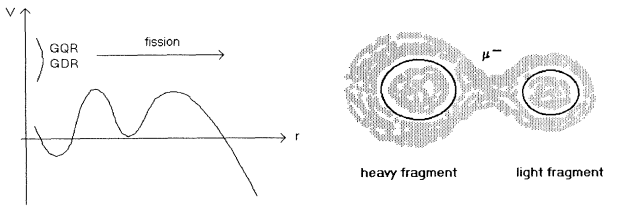

FIG. 2. Left side: double-humped fission barrier for an actinide nucleus; the giant dipole resonance (GDR) and giant quadrupole resonance (GQR) are the doorway states to fission. Right side: prompt fission in the presence of the muon.

ily understood in terms of a "correlation diagram" in which one plots the binding energies of the transient muonic molecule as a function of the internuclear distance R (Fig. 3). If the nuclear fission process is slow (large energy dissipation), the muon will stay in the lowest molecular energy level ($1s\sigma$) throughout the fission process and emerge in the $1s$ bound state of the heavy fission fragment. On the other hand, if the nuclear motion is relatively fast (low friction), there is a nonvanishing probability that the muon may be transferred to higher-lying molecular orbitals, e.g., the $2p\sigma$ level from where it may end up attached to the light fission fragment. Hence, theoretical studies of the muon-attachment probability to the light fission fragment in combination with experimental data can be utilized to probe the dynamics of prompt fission. In fact, the muon appears to be the only available tool for such studies. However, this simple picture is complicated by the fact that transitions to some of the higher-lying levels of the transient muonic molecule (e.g., $2p\pi$ and $2s\sigma$) result again in muon attachment to the heavy fragment.

To obtain an order-of-magnitude estimate for the muon attachment probabilities, we utilize a simple formula derived by Demkov [31] and by Meyerhof [32]. Their model is based on the two lowest molecular levels ($1s\sigma$ and $2p\sigma$) and utilizes first-order perturbation theory to calculate the transition probability from the $1s\sigma$ to the $2p\sigma$ level; within the two-level model, it is equal to the muon attachment probability to the light fission fragment:

$$P_L = \left(1 + e^{2|x|}\right)^{-1}, \quad x = \frac{\pi\,(I_H - I_L)}{\left(\frac{v}{c}\right)\sqrt{2m_\mu c^2}\left(\sqrt{I_H} + \sqrt{I_L}\right)}, \tag{3}$$

where I_H and I_L denote the binding energies of the muonic K shell belonging to the heavy and light fission fragments, respectively, and v is the relative velocity of the fission fragments. For a fragment charge asymmetry $\xi = Z_H/Z_L = 55/39 = 1.41$ (corresponding to the peak of the mass distribution) one finds I_H=5.93 MeV and I_L=3.45 MeV. If we assume that the molecular transition occurs at a relative velocity of the fission fragments of $v = 0.08c$, we obtain a muon attachment probability $P_L = 0.042$ for the light fission fragment; this value decreases to $P_L = 0.015$ if $v = 0.06c$.

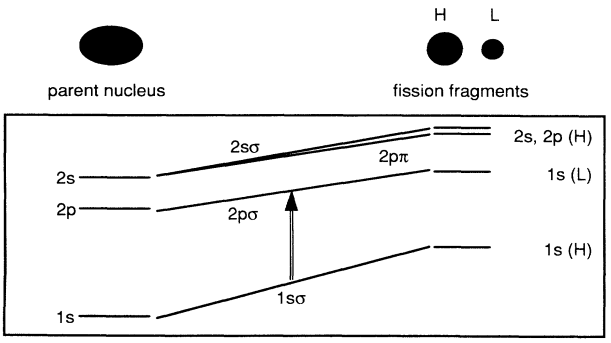

FIG. 3. Schematic "correlation diagram," i.e., binding energies of the transient muonic molecule as a function of the internuclear distance during prompt fission. At small distances (left side) the molecular energy levels correspond to the bound states of the $^{238}_{92}$U muonic atom; at large internuclear distances (right side) the molecular levels approach the binding energies of the heavy (H) and light (L) fission fragment.

III. MUON DYNAMICS: TIME-DEPENDENT DIRAC EQUATION

For the dynamical description of the muonic wave function during prompt fission, the electromagnetic coupling between muon and nucleus ($-e\gamma_\mu A^\mu$) is dominant; the weak interaction is negligible. The source of the electromagnetic vector potential A^μ is the nuclear current density $j^\mu_{\rm nuc}$. In the following we shall adopt a time-dependent description of the fission process, i.e., the current density of the fissioning nucleus is an explicit function of time $j^\mu_{\rm nuc} = j^\mu_{\rm nuc}(\mathbf{r}, t)$. Because of the nonrelativistic motion of the fission fragments ($v/c \approx 0.08$), retardation effects can be neglected and the electromagnetic interaction is dominated by the Coulomb interaction $A^0(\mathbf{r}, t)$; the vector potential $\mathbf{A}(\mathbf{r}, t)$ is several orders of magnitude smaller. We may determine the Coulomb potential generated by the nuclear charge density $\rho_{\rm nuc}(\mathbf{r}, t)$ either from Poisson's equation

$$\nabla^2 A^0(\mathbf{r}, t) = -4\pi\rho_{\rm nuc}(\mathbf{r}, t) \tag{4}$$

or, equivalently, from the Coulomb integral equation

$$A^0(\mathbf{r}, t) = \int d^3r' \frac{\rho_{\rm nuc}(\mathbf{r}', t)}{|\mathbf{r} - \mathbf{r}'|}. \tag{5}$$

It is convenient to measure the muon position in units of its Compton wavelength and to measure time in units of its Compton time. Hence we introduce the following dimensionless coordinates

$$\mathbf{x} = \mathbf{r}/\lambda_c\,, \quad \lambda_c = \hbar/(m_\mu c) = 1.87 \text{ fm},$$
$$\tau = t/\tau_c\,, \quad \tau_c = \lambda_c/c = 6.23 \times 10^{-24} \text{ s} \tag{6}$$

and the dimensionless Coulomb interaction between the muon and the fissioning nucleus

$$V^0 = -eA^0/(m_\mu c^2). \tag{7}$$

The muonic binding energy in the ground state of an actinide muonic atom amounts to 12% of the muonic rest mass; hence nonrelativistic calculations, while qualitatively correct, are limited in accuracy. Several years ago, we have demonstrated the feasibility of such nonrelativistic calculations [5,6,10,11] which are based on the Schrödinger equation

$$[-\tfrac{1}{2}\boldsymbol{\nabla}^2 + V^0(\mathbf{x}, \tau)]\phi(\mathbf{x}, \tau) = i\frac{\partial}{\partial\tau}\phi(\mathbf{x}, \tau). \tag{8}$$

Recently, we have developed the numerical methodology to solve the relativistic problem on a three-dimensional

Cartesian mesh. The time-dependent Dirac equation for the muonic spinor wave function in the Coulomb field of the fissioning nucleus has the form

$$[-i\boldsymbol{\alpha}\cdot\boldsymbol{\nabla}+\beta+V^0(\mathbf{x},\tau)]\psi(\mathbf{x},\tau)=i\frac{\partial}{\partial\tau}\psi(\mathbf{x},\tau). \quad (9)$$

Quantum electrodynamics radiative corrections such as vacuum polarization and self-energy amount to less than 1% in heavy muonic atoms [33] and are negligible in view of other uncertainties.

IV. FISSION DYNAMICS

A. Parametrization of nuclear shape and density

In these first numerical studies of the time-dependent Dirac equation for prompt muon-induced fission on a three-dimensional lattice, we have chosen a relatively simple parametrization of the nuclear charge distribution (see Fig. 4): two spherical segments (radii R_1, R_2) with uniform charge density separated at a distance R. Because of volume conservation during fission, the fragment radii depend upon the elongation, $R_i = R_i(R)$. In subsequent studies, more realistic charge density distributions will be obtained from the hydrodynamic model [34], from the shell correction method [35], or from nonrelativistic and relativistic mean-field theories [4,36,37]. The fission process is described by two collective coordinates: the fission coordinate R and a mass asymmetry parameter defined as $\xi = (R_1/R_2)^3$.

B. Fission mass parameter

Microscopic nuclear structure calculations, e.g., the cranking model [38], show that the collective mass parameter B associated with the fission coordinate R is not constant, but in fact a function of the distance R. In our current model calculation this behavior is taken into account: After the nucleus has reached the scission point $R_{\rm sci}$ we use the reduced mass $m_{\rm red}$ of the fission fragments

$$B(R \geq R_{\rm sci}) = m_{\rm red} = m\frac{A_1 A_2}{A_1 + A_2}, \quad (10)$$

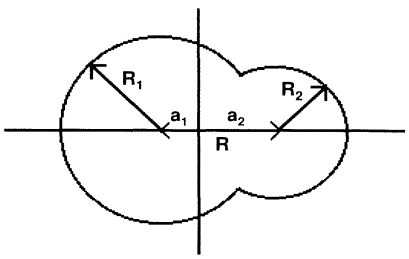

FIG. 4. Parametrization of the nuclear charge distribution: two spherical segments (radii R_1, R_2) with uniform charge density separated at a distance R.

where m denotes the nucleon mass. At small distances corresponding to the ground-state minimum of the actinide parent nucleus, we can determine $B(R)$ from the mass parameter $B(\beta)$ associated with the β vibrations. The collective model yields [39]

$$B(\beta_1) = \frac{\hbar^2}{\Delta E\,(2^+\beta \rightarrow 0^+\beta)\,\beta_1^2}, \quad (11)$$

where β_1 denotes the ground-state deformation and ΔE is the transition energy in the first β-vibrational band. For the nuclear shape parametrization given above, one finds the following relationship between the two mass parameters by simple geometric considerations

$$B(R_{\rm min}) = \frac{\pi B(\beta_1)}{5R_0^2}, \quad (12)$$

where $R_{\rm min}$ is the nuclear elongation in the ground-state minimum and $R_0 = (1.2\ {\rm fm})A^{1/3}$. For distances between $R_{\rm min}$ and $R_{\rm sci}$, $B(R)$ is obtained by linear interpolation between the values of these two mass parameters.

C. Fission potential

From experimental studies of fission induced by neutron capture or neutron transfer reactions one can map out the properties of the fission potential. We first construct an empirical fission potential $U(z)$ for a ficticious constant mass parameter; for convenience we utilize the reduced mass $m_{\rm red}$ of the fission fragments. Later on, we transform this potential to the coordinate-dependent mass $B(R)$. Following Back [40] we parametrize the double-humped fission potential with four parabolic sections

$$U(z) = \begin{cases} E_1 + \frac{1}{2}m_{\rm red}\omega_1^2(z-z_1)^2, & 0 \leq z \leq z_{1A}, \\ E_A - \frac{1}{2}m_{\rm red}\omega_A^2(z-z_A)^2, & z_{1A} \leq z \leq z_{A2}, \\ E_2 + \frac{1}{2}m_{\rm red}\omega_2^2(z-z_2)^2, & z_{A2} \leq z \leq z_{2B}, \\ E_B - \frac{1}{2}m_{\rm red}\omega_B^2(z-z_B)^2, & z_{2B} \leq z \leq z_3, \\ Z_H Z_L e^2/R(z) + {\rm const}, & z \geq z_3. \end{cases} \quad (13)$$

The four regions $i = 1, A, 2, B$ correspond to the first minimum, the inner barrier, the second minimum, and the outer barrier, respectively. At large distances, the parabolic potential is joined smoothly with the Coulomb potential of the fission fragments. If the ground-state energy is normalized to zero, the energy of the first minimum is given by $E_1 = -\frac{1}{2}E_{0^+\beta}$, where $E_{0^+\beta} = \hbar\omega_1$ is the position of the β-vibrational bandhead. As a specific example we consider here the isotope ^{238}U. We find $\hbar\omega_1 = 0.993$ MeV, from which we deduce $E_1 = -0.497$ MeV. The barrier heights and frequencies are taken from Table 2 of the review article by Bjornholm and Lynn [41]: $E_A = E_B = 5.70$ MeV, $\hbar\omega_A = 1.0$ MeV, $\hbar\omega_B = 0.60$

MeV. These authors also report the energy of the isomeric ground state to be $E_{\rm iso} = 2.60$ MeV. The curvature $\hbar\omega_2$ is probably the least certain parameter. From a fit to (t,p) reactions Back [40] finds $\hbar\omega_2 = 0.90$ MeV, from which we infer $E_2 = E_{\rm iso} - \frac{1}{2}\hbar\omega_2 = 2.15$ MeV for the value of the isomeric potential minimum. The ground-state deformation z_1 is obtained from the β-vibrational band, and the parameters of the parabolic sections (z_{1A}, z_A, z_{A2}, z_2, z_{2B}, z_B, and z_3) are obtained uniquely by requiring continuity of the potential $U(z)$ and its first derivative.

We now transform the potential $U(z)$ which corresponds to a constant mass parameter to the physical fission potential with coordinate dependent mass $B(R)$. Starting from the nuclear energy

$$E_{\rm nuc} = \frac{m_{\rm red}}{2}\left(\frac{dz}{dt}\right)^2 + U(z) \tag{14}$$

we obtain with the coordinate transformation $z = z(R)$:

$$E_{\rm nuc} = \frac{m_{\rm red}}{2}\left(\frac{dz}{dR}\frac{dR}{dt}\right)^2 + U(z(R))$$

$$= \frac{1}{2}B(R)\left(\frac{dR}{dt}\right)^2 + V_{\rm fis}(R). \tag{15}$$

The last equation determines the relationship between the fission coordinates R and z (for variable and constant mass, respectively)

$$dz = \sqrt{\frac{B(R)}{m_{\rm red}}}dR, \tag{16}$$

from which $z = z(R)$ can be obtained by integration, and it also defines the physical fission potential $V_{\rm fis}(R)$, which is shown in Fig. 5.

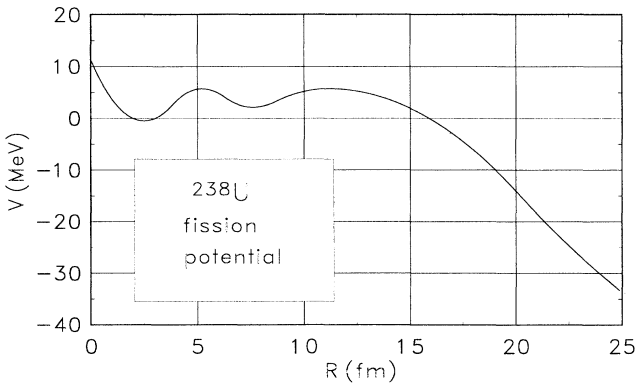

FIG. 5. Phenomenological fission potential for $^{238}_{92}$U corresponding to the coordinate-dependent mass parameter $B(R)$ defined in Sec. IV B. The potential is constructed from four parabolic sections and is smoothly joined with the Coulomb potential of the fission fragments at large distance R.

D. Fission mass asymmetry parameter

The phenomenological mass asymmetry parameter $\xi = (R_1/R_2)^3$ is made explicitly R dependent, $\xi = \xi(R)$, as indicated in Fig. 6. In this way, we reproduce the results of fission calculations in the shell correction method [35]: symmetric shapes, $\xi = 1$, up to the second minimum in the fission potential (E_2) and then a steady increase to the asymptotic value $\xi(R \to \infty) = A_H/A_L$ which is reached at the outer fission barrier (E_B).

E. Classical description of nuclear dynamics

Because the nuclear excitation energy exceeds the fission barrier height, there is no barrier tunneling and we may treat the fission dynamics classically; in this case, the collective nuclear energy has the form

$$E^{\rm eff}_{\rm nuc} = \frac{1}{2}B(R)\left(\frac{dR}{dt}\right)^2 + V_{\rm eff}(R). \tag{17}$$

The effective fission potential

$$V_{\rm eff}(R) = V_{\rm fis}(R) + E_\mu(R) \tag{18}$$

contains a contribution from the muonic binding energy which depends on the elongation of the fissioning nucleus. This results in an augmentation of the fission barrier, an interesting effect first studied by Leander and Möller [42]. In addition, we introduce a linear friction force which acts between the outer fission barrier and the scission point. In this case, the dissipation function D is a simple quadratic form in the velocity and the time rate of change of the nuclear collective energy equals twice the dissipation function

$$\frac{dE^{\rm eff}_{\rm nuc}}{dt} = -2D = -f\left(\frac{dR}{dt}\right)^2. \tag{19}$$

The adjustable friction parameter f determines the dissipated energy. The classical collective motion of the

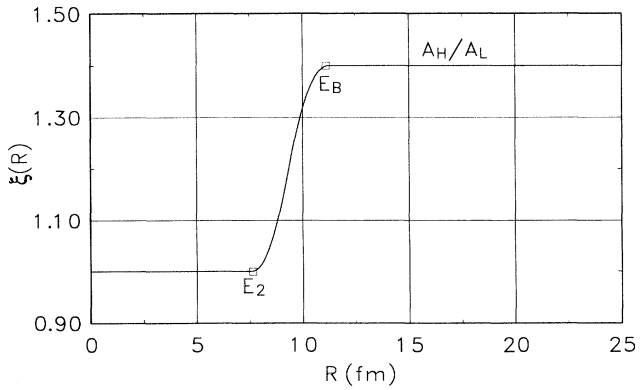

FIG. 6. Fission mass asymmetry parameter as function of the fission coordinate R.

fissioning nucleus is described by Eqs. (17)–(19). Note that the nuclear and muonic motions are coupled via the instantaneous muon energy

$$E_\mu(R(t)) = \langle \psi(\mathbf{x},t) \left| -i\boldsymbol{\alpha}\cdot\boldsymbol{\nabla} + \beta + V^0(\mathbf{x},t) \right| \psi(\mathbf{x},t)\rangle . \tag{20}$$

Therefore, the nuclear equation of motion (19) and the Dirac equation (9) must be solved simultaneously.

V. ELECTROMAGNETIC INTERACTION BETWEEN MUON AND NUCLEUS

The Coulomb interaction is computed numerically from the nuclear charge distribution $\rho_{\rm nuc}(\mathbf{r},t)$ of the fissioning nucleus. For the axially symmetric nuclear charge distribution considered here, it is advantageous to introduce cylindrical coordinates

$$-eA^0(z,\rho,t) = 4\int_0^\infty \rho' d\rho' \int_{-\infty}^{\infty} dz' \rho_{\rm nuc}(z',\rho',t)\,\frac{F\left(\frac{\pi}{2},k\right)}{\sqrt{a+b}}, \tag{21}$$

where $F\left(\frac{\pi}{2},k\right)$ denotes the complete elliptic integral of the first kind and

$$a = \rho^2+\rho'^2+(z-z')^2, \quad b = 2\rho\rho', \quad k = \sqrt{\frac{2b}{a+b}}. \tag{22}$$

As long as the fission fragments are connected, the double integral must be solved numerically on a two-dimensional equidistant mesh for the coordinates (z',ρ') with a step size $\Delta z' = \Delta\rho' = 0.25\lambda_c = 0.47$ fm. However, once the fission fragments have separated ($R > R_1 + R_2$) we can solve the Coulomb integral analytically because of the simple geometry of the nuclear charge distribution; we find

$$\begin{aligned} -eA^0(z,\rho,t) = &-(Z_H\alpha) f\big(d_1(t), R_H\big) \\ &-(Z_L\alpha) f\big(d_2(t), R_L\big), \end{aligned} \tag{23}$$

where Z_H, Z_L and R_H, R_L denote the charge numbers and radii of the heavy and light fission fragments, respectively. The distances d_1, d_2 are given by

$$\begin{aligned} d_1(t) &= \sqrt{\rho^2+[z+a_1(t)]^2}\,, \\ d_2(t) &= \sqrt{\rho^2+[z-a_2(t)]^2}. \end{aligned} \tag{24}$$

The geometric quantities $a_i(t)$ are depicted in Fig. 4, and the function f is defined by

$$f(r,R) = \begin{cases} \frac{1}{r}\,, & r > R, \\ \frac{1}{2R}\left(3-\frac{r^2}{R^2}\right), & r < R. \end{cases} \tag{25}$$

VI. NUMERICAL IMPLEMENTATION

We solve the time-dependent Dirac equation (9) on a three-dimensional Cartesian lattice using the basis-spline collocation method. The four Dirac spinor components $\psi^{(p)}(x,y,z,\tau), p = (1,2,3,4)$ are expanded in terms of a product of basis-spline functions $B_i^M(x)$

$$\psi^{(p)}(x,y,z,\tau) = \sum_{i,j,k} B_i^M(x) B_j^M(y) B_k^M(z) \psi_{(p)}^{ijk}(\tau). \tag{26}$$

The basis-spline functions $B_i^M(x)$ are piecewise-continuous polynomials of order $(M-1)$. They represent generalizations of the "finite elements" that are widely used in computational physics; in fact, finite elements are B-splines with $M = 2$. In the present calculations we employ B-splines of order $M \geq 5$. Since the spinor wave function is represented by polynomials of high order, very high accuracy can be achieved with a modest number of lattice points. This is the crucial advantage of the B-spline collocation method which enables us to study three-dimensional problems.

In the collocation method, the unknown expansion coefficients $\psi_{(p)}^{ijk}(\tau)$ are eliminated as follows: the Dirac spinor components $\psi^{(p)}$ are represented on a rectangular Cartesian lattice $(x_\alpha, y_\beta, z_\gamma)$

$$\psi_{\alpha\beta\gamma}^{(p)} = \psi^{(p)}(x_\alpha,y_\beta,z_\gamma,\tau) = \sum_{i,j,k} B_i^M(x_\alpha) B_j^M(y_\beta) B_k^M(z_\gamma) \psi_{(p)}^{ijk}(\tau) = \sum_{i,j,k} B_{\alpha i}^M B_{\beta j}^M B_{\gamma k}^M \psi_{(p)}^{ijk}(\tau), \tag{27}$$

where $(\alpha = 1,\ldots,N_x; \beta = 1,\ldots,N_y; \gamma = 1,\ldots,N_z)$, i.e., the lattice representation of the spinor wave function $\psi^{(p)}$ is a vector $\boldsymbol{\psi}$ in collocation space with $N = 4N_xN_yN_z$ complex components. Even for lattices of moderate size N becomes quite large. For example, if $N_x = N_y = N_z = 29$ we find a wave vector of dimension $N = 9.8\times 10^4$. By matrix inversion of the last equation we find the relation

$$\psi_{(p)}^{ijk} = \sum_{\alpha,\beta,\gamma} B_M^{i\alpha} B_M^{j\beta} B_M^{k\gamma} \psi_{\alpha\beta\gamma}^{(p)}, \tag{28}$$

which allows us to eliminate the coefficients of the basis expansion in favor of the values of the Dirac spinor wave function at the collocation points. In the B-spline collocation method, the original partial differential equation (9) is transformed into a matrix equation

$$\mathbf{H}\boldsymbol{\psi}(\tau) = i\frac{\partial\boldsymbol{\psi}}{\partial\tau}, \tag{29}$$

where we use boldface type for matrices and vectors in collocation space. The lattice representation of the Dirac Hamiltonian is a $N\times N$ matrix $\mathbf{H}$ of the form

$$\mathbf{H} = -i\boldsymbol{\alpha}\cdot\mathbf{D} + \beta + \mathbf{V}^0(\mathbf{x},\tau). \tag{30}$$

It is impossible to store $\mathbf{H}$ in computer memory, since this would require the storage of N^2 complex double-precision numbers. Even for the moderate lattice size mentioned above one obtains $N^2 = 9.6 \times 10^9$. Hence, we must resort to iterative methods for the solution of the matrix equation which do not require the storage of $\mathbf{H}$.

We solve the time-dependent Dirac equation in two steps. First, we consider the static Coulomb problem at time τ=0, i.e., the muon bound to an actinide nucleus. The stationary Dirac equation for the ground-state spinor is given by

$$\mathbf{H}_0 \psi_{gs} = E_{gs} \psi_{gs} \tag{31}$$

with the Hamiltonian

$$\mathbf{H}_0 = \mathbf{H}(\tau = 0). \tag{32}$$

The static problem is solved by the iterative procedure (damped relaxation method [43])

$$\psi_{gs}^{(i+1)} = \psi_{gs}^{(i)} + \Delta t \cdot \mathcal{D}(\mathbf{H}_0 - \langle \psi_{gs}^{(i)} | \mathbf{H}_0 | \psi_{gs}^{(i)} \rangle) \psi_{gs}^{(i)} \tag{33}$$

with the damping operator

$$\mathcal{D} = \left(\frac{-i\boldsymbol{\alpha} \cdot \mathbf{D}}{\mu} + \beta + \nu \right)^{-1}. \tag{34}$$

The parameters μ and ν may be thought of as mass and energy shifts, respectively. For $^{238}_{92}$U we utilize the parameters $\mu = 3.0$, $\nu = -0.74$, $\Delta t = 4.5$.

The second part of our numerical methodology is the solution of the time-dependent Eq. (29) by a Taylor expansion of the propagator. For an infinitesimal time step $\Delta\tau$ we find

$$\begin{aligned} \psi(\tau + \Delta\tau) &= \mathbf{U}(\tau + \Delta\tau, \tau)\, \psi(\tau) \\ &\approx \left(1 + \sum_{n=1}^{N} \frac{(-i\Delta\tau \mathbf{H})^n}{n!} \right) \psi(\tau). \end{aligned} \tag{35}$$

We have thus reduced the original problem to a series of (matrix)×(vector) operations which can be executed with high efficiency on vector or parallel supercomputers without explicitly storing the matrix in memory. Details of the numerical method can be found in Refs. [44–47]. Typical runs on a CRAY-2 supercomputer for cubic or rectangular lattices with up to 29 points in the x, y, and z directions and a lattice spacing $\Delta x = 2.0\lambda_c$ take four Megawords of memory and 6.5 CPU hours. As in all lattice calculations, we need to demonstrate convergence in terms of the lattice size and lattice spacing; we estimate that convergent calculations will require a rectangular lattice with approximately $39 \times 39 \times 65$ lattice points and a lattice spacing $\Delta x \approx 1.0\lambda_c$. We also plan to examine a possible additional improvement of our numerical method by using variable lattice spacing; the basis-spline collocation method is well suited to this task.

VII. NUMERICAL RESULTS AND DISCUSSION

In the following we present results for prompt fission of ^{238}U induced by the $E2 : (3d \rightarrow 1s, 9.6\ \text{MeV})$ nonradiative muonic transition. Figure 7 shows the relative velocity of the fission fragments as a function of time; all times are indicated in units of the muon Compton time τ_C, Eq. (6). Our model assumes that there is no friction until the outer fission barrier E_B is reached; hence, the velocity profile is essentially the mirror image of the fission potential displayed in Fig. 5, with small deviations arising from muonic binding energy contributions. The numerical calculations have been carried out for a variety of friction parameters; for $f = 500$ we observe a time delay in the nuclear relative motion of $\Delta t_{\text{nuc}} \cong 600\tau_c = 3.7 \times 10^{-21}$ s.

Figure 8 shows the nuclear energy dissipation (in form of neutron and γ emission) as a function of time; in our model, friction is confined to the region between the outer fission barrier and the scission point; for friction parameters $f = 10$ and $f = 500$, we obtain total dissipated energies $E_{\text{diss}} = 0.7$ MeV and 15.8 MeV, respectively.

In Fig. 9 we depict the time variation of the instantaneous muon energy defined in Eq. (20): at $t = 0$, it corresponds to the energy of a muon bound by the Coulomb field of a quadrupole-deformed ^{238}U nucleus; at $t \rightarrow \infty$, the binding energy approaches a value somewhere in between the binding energies of the heavy and the light fission fragment, but much closer to that of the heavy fragment.

Figure 10 shows the Coulomb interaction energy between the muon and the fission fragments at large separation. The two Coulomb wells are clearly visible; the deeper well on the left is generated by the heavy fission fragment. Also shown (at the bottom of Fig. 10) is the associated muon position probability density [13]. For a fragment mass asymmetry $A_H/A_L = 1.40$ we observe that the muon sticks predominantly to the heavy fragment; the muon attachment probability to the light fragment is represented by the small bump on the right.

The process of prompt muon-induced fission was first observed experimentally by Diaz *et al.* [48]. More recent experiments by Ahmad *et al.* [21] yield a total fission probability per muon stop of $P_f = 0.068$ for ^{238}U and a ratio $P_f(\text{prompt})/P_f(\text{delayed}) = 0.089$. Mean lifetimes of muons bound to fission fragments of several actinides have been measured by Schröder *et al.* [15]. From the observed lifetime $\tau_\mu = 1.30 \times 10^{-7}$ s it was deduced that

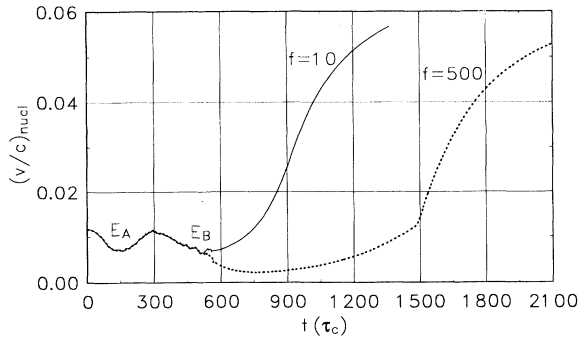

FIG. 7. Fission fragment velocity versus time for two values of the friction parameter, $f = 10$ and $f = 500$.

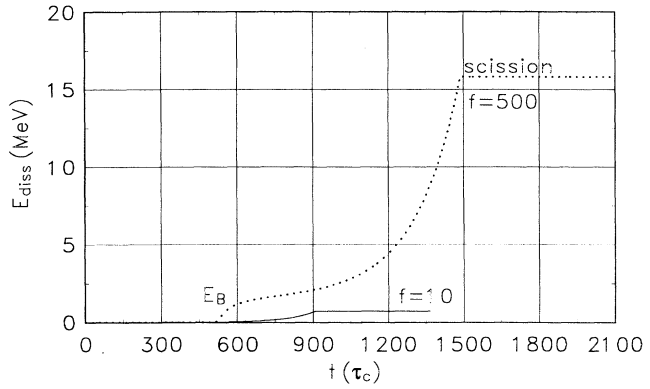

FIG. 8. Energy dissipated during fission, for $f = 10$ and $f = 500$.

the muon is predominantly captured by the heavy fragment with a probability $P_H \geq 0.9$. The most recent experimental muon attachment results are given by Polikanov [20]: (0.090 ± 0.027) for a fission mass asymmetry $\xi = 1.13$, and (0.015 ± 0.15) for a fission mass asymmetry $\xi = 1.90$.

Based on the formalism presented here, preliminary results for the muon attachment probability to the light fission fragment P_L as a function of the dissipated nuclear energy have been published in a recent Letter journal [13]. As expected, we found that P_L decreases with dissipated energy. For a fission mass asymmetry $\xi = 1.40$ (which corresponds to the peak of the fission mass distribution in ^{238}U) and reasonable values of the dissipated energy, we calculate muon attachment probabilities P_L less than 10%. This is in agreement with the data of Schröder *et al.* [15]. Since the sticking probability depends strongly on the fragment mass, a quantitative comparison with the data [20] is not yet possible. For this purpose, we have to replace the empirical fission potential used in this work (which is valid only for $\xi = 1.40$) with a theoretical fission potential energy surface that is explicitly mass-asymmetry dependent.

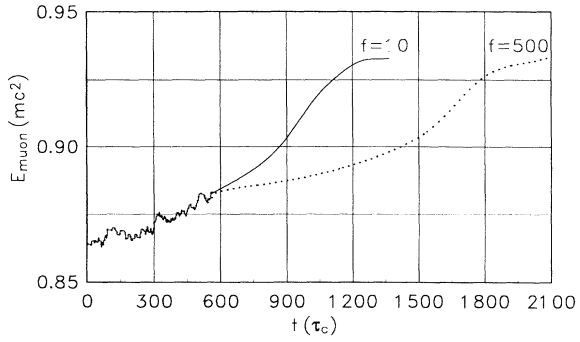

FIG. 9. Expectation value of the instantaneous muon energy during fission, for $f = 10$ and $f = 500$.

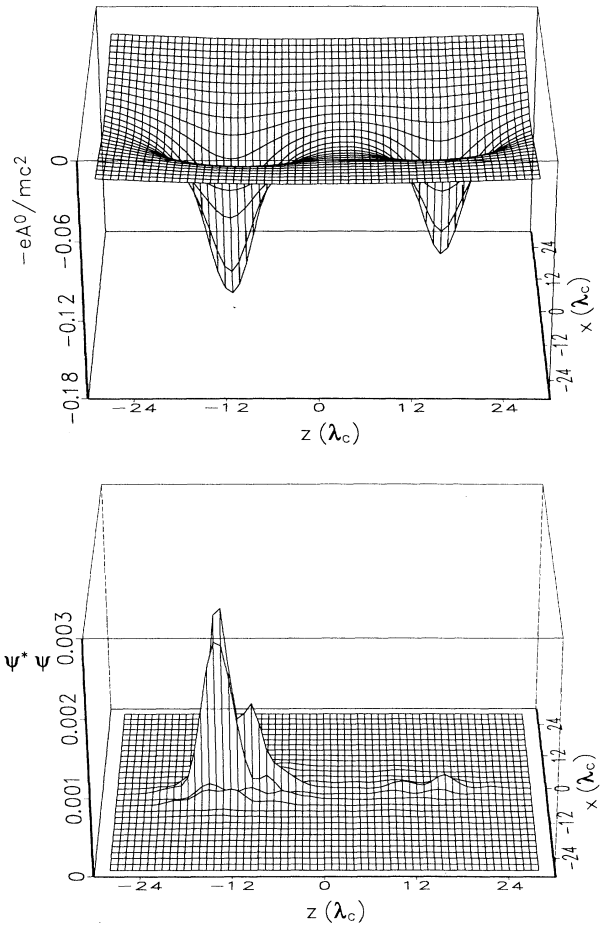

FIG. 10. Coulomb potential (top) and muon position probability density (bottom) at time $t = 1301\tau_c$ and internuclear distance $R = 52.9$ fm. The friction parameter $f = 10$ corresponds to $E_{diss} = 0.7$ MeV.

VIII. OUTLOOK

Prompt muon-induced fission is a very promising tool for the study of nuclear fission dynamics. In particular, our goal is to determine the nuclear energy dissipation between the outer fission barrier and the scission point; this will be possible in the near future by comparing our theoretical values for the muon attachment probabilities as a function of energy dissipation with the experimental data [20].

In this paper we have presented a dynamical theory of prompt muon-induced fission. For the first time, the muon dynamics is described by the Dirac equation (rather than the nonrelativistic Schrödinger equation) with a time-dependent external Coulomb field which is generated by the fission fragments in motion. Because the nuclear excitation energy exceeds the fission barrier height, it is permissible to treat the fission dynamics classically, including a phenomenological friction force.

We have presented both the formalism and the nu-

merical methodology in considerable detail; it is our intent to build a robust time-dependent model, and the present paper is only one first important step along the way. It will serve as a foundation for future work; in particular, we plan to extend the present nuclear dynamics description as follows: We want to examine the dependence of the muon final state on different theoretical descriptions of the nuclear density distributions and fission potentials, e.g., the hydrodynamic model [34], the shell-correction method [35], and the nonrelativistic and relativistic mean-field theories [4,36,37]. Ultimately, we want to link our current studies of the time-evolution of the muonic spinor wave function to a microscopic treatment of fission dynamics. This can be achieved via a time-dependent Hartree-Fock description [4] of the nuclear motion between the outer fission barrier and the scission point, providing the first experimentally accessible way to check the concept of mean-field dynamics and the associated one-body dissipation. Discrepancies between theory and experiment would indicate two-body dissipation.

It will be interesting to compare the muon attachment results to experimental information from other methods such as neutron emission [49] and to theoretical models of friction (macroscopic and microscopic) [3,34,50,51]. In this context we plan to study μ^- attachment probabilities to the fission fragments as a function of dissipated energy and fission fragment mass asymmetry, and we will attempt to analyze all available experimental data. We also plan to make theoretical predictions for actinide nuclei which have not yet been investigated experimentally.

ACKNOWLEDGMENTS

This research project was sponsored in part by the U.S. Department of Energy under Contract No. DE-FG05-87ER40376 with Vanderbilt University, and under Contract No. DE-AC05-84OR21400 with Oak Ridge National Laboratory managed by Martin Marietta Energy Systems. In addition, this research project was partially supported by the U.S. Department of Energy High Performance Computing and Communications Program (HPCC) as the "Quantum Structure of Matter Grand Challenge" project. The numerical calculations were carried out using CRAY-2 supercomputers at the National Center for Supercomputing Applications in Illinois and the National Energy Research Supercomputing Center at Lawrence Livermore National Laboratory, and using the Intel iPSC/860 hypercube multicomputer at the Oak Ridge National Laboratory. Two of the authors (V.E.O. and J.A.M.) acknowledge travel support from the NATO Collaborative Research Grants Program.

[1] Y.N. Kim, *Mesic Atoms and Nuclear Structure* (North-Holland, Amsterdam, 1971).
[2] J.M. Eisenberg and W. Greiner, *Nuclear Theory, Vol. 2: Excitation Mechanisms of the Nucleus* (North-Holland, Amsterdam, 1970).
[3] R.W. Hasse, Rep. Prog. Phys. **41,** 1027 (1978).
[4] A.S. Umar and M.R. Strayer, Comput. Phys. Commun. **63,** 179 (1991).
[5] J.A. Maruhn, V.E. Oberacker, and V. Maruhn-Rezwani, Phys. Rev. Lett. **44**, 1576 (1980).
[6] V.E. Oberacker and J.A. Maruhn, in Proceedings of the International Conference on Nuclear Physics, Berkeley, California, 1980, Abstracts, Report No. LBL-11118 (unpublished), p. 854.
[7] Z.Y. Ma, X.Z. Wu, G.S. Zhang, Y.C. Cho, Y.S. Wang, J.H. Chiou, S.T. Sen, F.C. Yang, and J.O. Rasmussen, Nucl. Phys. **A348**, 446 (1980).
[8] P. Olanders, S.G. Nilsson, and P. Möller, Phys. Lett. **90B**, 193 (1980).
[9] Z. Ma, X. Wu, J. Zhang, Y. Zhuo, and J.O. Rasmussen, Phys. Lett. **106B**, 159 (1981).
[10] V.E. Oberacker and J.A. Maruhn, in Proceedings of the LAMPF II Workshop, Los Alamos, New Mexico, 1982, Report No. LA-9572-C (unpublished), Vol. 2, p. 422.
[11] V.E. Oberacker, in *Proceedings of the International Symposium on Nuclear Fission and Heavy-Ion Induced Reactions*, Rochester, New York, 1986 (Harwood, New York, 1987), p. 113.
[12] V.E. Oberacker, A.S. Umar, J.C. Wells, M.R. Strayer, and C. Bottcher, *Supercomputing 91,* Albuquerque, New Mexico, 1991 (IEEE Computer Society Press, Los Alamitos, CA, 1991), Final Program, p. 89.
[13] V.E. Oberacker, A.S. Umar, J.C. Wells, C. Bottcher, and M.R. Strayer, Phys. Lett. B **293**, 270 (1992).
[14] W.W. Wilcke, M.W. Johnson, W.U. Schröder, J.R. Huizenga, and D.G. Perry, Phys. Rev. C **18**, 1452 (1978).
[15] W.U. Schröder, W.W. Wilcke, M.W. Johnson, D. Hilscher, J.R. Huizenga, J.C. Browne, and D.G. Perry, Phys. Rev. Lett. **43**, 672 (1979).
[16] A. Gavron, in "Physics with LAMPF II," Los Alamos National Laboratory Proposal No. LA-9798-P, 1983 (unpublished), p. 126.
[17] Dz. Ganzorig, P.G. Hansen, T. Johansson, B. Jonson, J. Konijn, T. Krogulski, V.D. Kuznetsov, S.M. Polikanov, G. Tibell, and L. Westgaard, Phys. Lett. **77B**, 257 (1978).
[18] T. Johansson, J. Konijn, T. Krogulski, S. Polikanov, H.W. Reist, and G. Tibell, Phys. Lett. **97B**, 29 (1980).
[19] S. Polikanov, in *Proceedings of the International Summer School on Nuclear Structure*, Dronten, The Netherlands, 1980 (Plenum, New York, 1981), p. 355.
[20] S. Polikanov, Nucl. Phys. **A502,** 195c (1989).
[21] S. Ahmad, G.A. Beer, M.S. Dixit, J.A. MacDonald, G.R. Mason, A. Olin, R.M. Pearce, O. Häusser, and S.N. Kaplan, Phys. Lett. **92B**, 83 (1980).
[22] S.N. Kaplan *et al.*, in [6], p. 370.
[23] E. Fermi and E. Teller, Phys. Rev. **72**, 399 (1947).
[24] C.S. Wu and L. Wilets, Annu. Rev. Nucl. Sci. **19**, 527 (1969).
[25] B. Goulard and H. Primakoff, Phys. Rev. C **10**, 2034 (1974).
[26] J.A. Wheeler, Rev. Mod. Phys. **21**, 133 (1949).
[27] D.F. Zaretski and V.M. Novikov, Nucl. Phys. **28**, 177 (1961).

[28] B.L. Berman and S.C. Fultz, Rev. Mod. Phys. **47**, 713 (1975).
[29] A. Neto *et al.*, Phys. Rev. C **18**, 863 (1978).
[30] E. Teller and M.S. Weiss, "Is the Muon a Multipole Meter?" Report No. UCRL-83616, 1979 (unpublished), prepared for the Maurice Goldhaber Festschrift.
[31] Yu.N. Demkov, Zh. Eksp. Teor. Fiz. **45**, 195 (1963) [Sov. Phys. JETP **18**, 138 (1964)].
[32] W.E. Meyerhof, Phys. Rev. Lett. **22,** 1341 (1973).
[33] E. Borie and G.A. Rinker, Rev. Mod. Phys. **54,** 67 (1982).
[34] K.T.R. Davies, A.J. Sierk, and J.R. Nix, Phys. Rev. C **13**, 2385 (1976).
[35] S. Åberg, H. Flocard, and W. Nazarewicz, Annu. Rev. Nucl. Part. Sci. **40,** 439 (1990).
[36] S.J. Lee, J. Fink, A.B. Balantekin, M.R. Strayer, A.S. Umar, P.G. Reinhard, J.A. Maruhn, and W. Greiner, Phys. Rev. Lett. **60,** 163 (1988).
[37] V. Blum, J. Fink, P.G. Reinhard, J.A. Maruhn, and W. Greiner, Phys. Lett. B **223**, 123 (1989).
[38] P. Ring and P. Schuck, *The Nuclear Many-Body Problem* (Springer, New York, 1980).
[39] J.M. Eisenberg and W. Greiner, *Nuclear Theory, Vol. 1: Nuclear Models* (North-Holland, Amsterdam, 1970).
[40] B.B. Back, Nucl. Phys. **A228**, 323 (1974).
[41] S. Bjornholm and J.E. Lynn, Rev. Mod. Phys. **52**, 725 (1980).
[42] G. Leander and P. Möller, Phys. Lett. **57B**, 245 (1975).
[43] C. Bottcher, M.R. Strayer, A.S. Umar, and P.G. Reinhard, Phys. Rev. A **40**, 4182 (1989).
[44] A.S. Umar, J.-S. Wu, M.R. Strayer, and C. Bottcher, J. Comp. Phys. **93,** 426 (1991).
[45] J.C. Wells, V.E. Oberacker, A.S. Umar, C. Bottcher, M.R. Strayer, and J.S. Wu, in *Proceedings of the International Conference on Computational Quantum Physics*, Vanderbilt University, Nashville, Tennessee, 1991, edited by A.S. Umar and V.E. Oberacker, AIP Conf. Proc. No. 260 (AIP, New York, 1992), p. 215.
[46] J.C. Wells, V.E. Oberacker, A.S. Umar, C. Bottcher, M.R. Strayer, J.-S. Wu, and G. Plunien, Phys. Rev. A **45**, 6296 (1992).
[47] J.C. Wells, A.S. Umar, V.E. Oberacker, C. Bottcher, M.R. Strayer, J.-S. Wu, J. Drake, and R. Flanery, Int. J. Mod. Phys. C **4**, 459 (1993).
[48] J.A. Diaz *et al.*, Nucl. Phys. **40**, 54 (1963).
[49] A. Gavron, A. Gayer, J. Boissevain, H.C. Britt, T.C. Awes, J.R. Beene, B. Cheynis, D. Drain, R.L. Ferguson, F.E. Obenshain, F. Plasil, G.R. Young, G.A. Petitt, and C. Butler, Phys. Rev. C **35,** 579 (1987).
[50] B.W. Bush, G.F. Bertsch, and B.A. Brown, Phys. Rev. C **45,** 1709 (1992).
[51] D. Kiderlen, H. Hofmann, and F.A. Ivanyuk, Nucl. Phys. (to be published).